# SENSITIVITY AND TOLERANCE STUDY FOR THE SwissFEL

Bolko Beutner*, Sven Reiche
Paul Scherrer Institut, 5232 Villigen PSI, Switzerland

*Abstract*

The SwissFEL facility will produce coherent, ultra-bright, and ultra-short photon pulses covering a wavelength range from 0.1 nm to 7 nm, requiring an emittance between 0.18 to 0.43 mm mrad. The facility consists of an S-band rf-gun and booster and a C-band main linac, which accelerates the beam up to 5.8 GeV. Two compression chicanes will provide a nominal peak current of about 3 kA. An important issue is the stability of the photon pulses leaving the undulator toward the user stations. Arrival time and peak current stability are crucial factors for the scientific return of the user experiments. Machine stability, especially the RF jitter, will directly affect these important figures. Shot-to-shot jitter is of main interest here since slow drifts can be compensated by slow feedback systems. We present here a study on stability including RF tolerances for a new optimised layout of the SwissFEL.

## INTRODUCTION

An important factor for FEL user facilities is the stability of the photon pulses at the user stations. Shot-to-shot jitter, as well as long-term drifts of machine parameters, such as rf phases and amplitudes, can sensibly affect the FEL performance. Most long-term drifts, e.g. by temperature changes, can be compensated for by feedback systems. For this reason the main concerns regarding performance are shot-to-shot fluctuations of various subsystems.

The FEL performance depends on the stability of certain subsystems $i$. This dependence of final beam parameters on variation in the subsystem $i$ is called sensitivity $S_i$. We consider only small variations and thus only consider the linear term of the sensitivity. The sensitivities describe how a bunch parameter $A$, such as peak current, varies caused by an upstream machine parameter $i$. From the sensitivity analysis and the given stability goals $\bar{\sigma}_A$, the tolerance for the subsystem $i$ can be calculated. It holds

$$\bar{\sigma}_i = \frac{\bar{\sigma}_A \sqrt{N_i}}{S_i}, \tag{1}$$

assuming $i$ is the only deviating property. Most systems contain more than one independent error source for a subsystem like klystrons in a linac section. Their number $N_i$ relaxes the corresponding tolerance by $\sqrt{N_i}$. In reality all systems contribute to the overall jitter $\sigma_A$ at the end of the machine and the tolerance for a subsystem must be smaller. This jitter

$$\sigma_A = \sqrt{\sum_i \frac{\sigma_i^2 S_i^2}{N_i}} \tag{2}$$

depends on the stability of all subsystems $\sigma_i$, which should not exceed the stability goal $\bar{\sigma}_A$. Tolerances $\sigma_i$ are tighter in this general case allowing jitter of all subsystems. With

$$\sigma_i = a_i \bar{\sigma}_i \tag{3}$$

and Eq. 2 $a_i$ has to fulfil

$$\sum_i a_i^2 \leq 1. \tag{4}$$

A complete set of tolerances is defined together with the subsystem experts. Such an optimisation is beyond the scope of this paper.

## OPTIMISED LAYOUT OF SWISSFEL

The basic layout of SwissFEL is summarised in Fig. 1. In this paper we focus on the 200pC operation mode. A detailed description of the reference design is given in [2] and [1]. However the design presented there requires very tight tolerances for the RF systems, which are challenging to fulfil with the state-of-art technology. We discuss in this paper a modified layout of the SwissFEL to relax these requirements on the RF systems, using the same hardware as for the CDR reference design.

In this optimisation of RF tolerances we focussed on a redistribution of chirp generation. In the CDR design a major fraction of the longitudinal energy chirp is generated in the S-band booster 2. This chirp dominates the compression factor in both chicanes, therefore a jitter in the S-band section has a strong effect on the final compression.

The strategy to relax tolerances here is to remove the chirp generated in booster 2 with the longitudinal wake fields in C-band linac 1. This requires a matching of the wake field generated chirp with the RF chirp and the required compression factors. In such a configuration additional chirp has to be generated in linac 1 for compression in BC2, which leads to a decoupling of the two compressions. To achieve this the beam energy at BC1 has to be reduced while the $R_{56}$ of BC1 is increased. Booster 1 is operated closer to on-crest phase while linac 1 is more off-crest than before. In this setup the compression factor in BC1 is smaller than in the reference design - this could be compensated by a higher $R_{56}$ in BC1 but we chose to mainly increase the chirp for BC2 to mitigate CSR effects. The resulting energy loss in linac 1 is compensated by higher gradients and on crest acceleration in linac 2 and 3. A summary of the parameters is given in Table 1.

Start-to-end simulations confirmed the feasibility of the new working point. In total the emittance, peak current and thus SASE performance is comparable. Differences are a

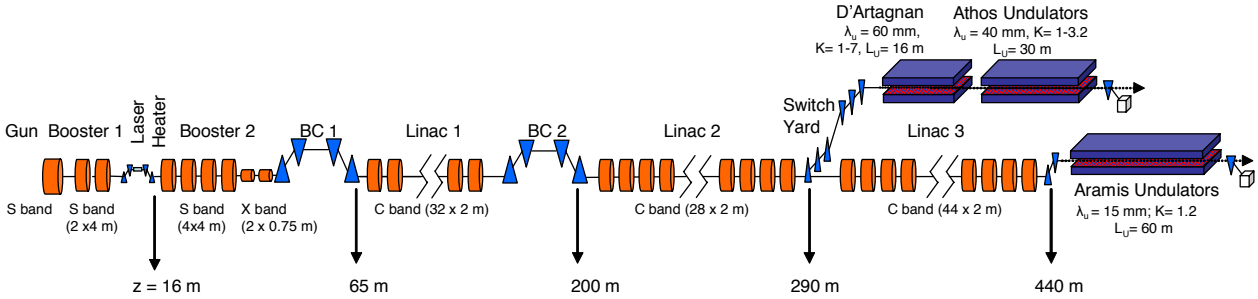


Figure 1: Layout of the SwissFEL. After an S-band gun and booster section a two stage compression scheme is used with an X-band phase space linariser. Three C-band linac sections are used. One between the chicanes and two main acceleration linacs downstream of BC2.

Table 1: SwissFEL machine parameters. A comparison between the 200pC reference design (right) and the new optimised design. Both layouts share the same hardware.

| | New Layout | CDR Layout |
|---|---|---|
| Booster 2 Phase | -17 deg | -20.5 deg |
| Booster 2 Amplitude | 16 MV/m | 20MV/m |
| X-band Phase | 180.13 deg | 180 deg |
| X-band Amplitude | 16.98 MV/m | 19.5 MV/m |
| Linac 1 Phase | -20.9 deg | -9.8 deg |
| Linac 1 Amplitude | 26.5 MV/m | 26 MV/m |
| Linac 2/3 Phase | 0 deg | +6 deg |
| Linac 2/3 Amplitude | 26.5 MV/m | 26 MV/m |
| BC1 | 4.2 deg | 3.82 deg |
| BC2 | 2.15 deg | 2.15 deg |
| Energy at BC1 | 355 MeV | 410 MeV |
| Energy at BC2 | 2.04 GeV | 2.1 GeV |
| Energy at Switchyard | 2.1 - 3.4 GeV | 2.1 - 3.4 GeV |
| Energy at Aramis | 5.8 GeV | 5.8 GeV |
| Bunch length at gun | 838.6 $\mu$m | 838.6 $\mu$m |
| Bunch length at BC1 | 124.2 $\mu$m | 72.7 $\mu$m |
| Bunch length at BC2 | 6.2 $\mu$m | 8.7 $\mu$m |

longitudinal more uniform pulse mainly attributed to a fine tuned X-band phase and a slightly larger FEL bandwidth due to the missing active compensation of the residual chirp at the end of the linacs. However, this effect on the FEL bandwidth is still in acceptable limits.

## SIMULATIONS

The sensitivities are obtained by a series of tracking runs from the injector to the undulator entrance. The problem is divided in two parts. Beam dynamics from the gun to the laser heater (at 130MeV) were studied with ASTRA [4]. These results are not discussed in detail in this paper. Most interesting for the bunch compression layout is the high energy section downstream of the invariant envelope matching regime. Elegant [5] is used for start-to-end calculations between the laser heater and the Aramis undulator entrance.

A set of parameters such as the magnet strength in BC 1 or the RF phase offsets are varied in a certain interval around the nominal settings. The resulting beam parameters at the undulator are then evaluated as a function of the individual deviated parameter. In this study the Fluctuations of the S- and X-band phase offset and amplitude (SBP, SBA, XBP, and XBA), the C-band linac 1 to 3 phases and amplitudes (L1P, L1A, L2P, L2A, L3P, and L3A), the bunch charge, injection time, and energy at the laser heater (LHQ, LHt, and LHE), and the bending angles of the chicanes (BC1 and BC2) are investigated. The linear term of polynomial fits to these dependencies are used as the sensitivities. Since the tightest tolerances are expected from the hard X-ray line, only the performance goals of the Aramis undulator are being studied in detail.

The sensitivities of components between the laser heater and the Aramis line are summarized in Table 2. This sensitivities are the linear slope around the reference working point. To estimate the jitter of a beam parameter at the undulator entrance the expected component jitter is multiplied by the given number, for example: A change of the S-band Phase by 0.1 degree will change the arrival time by -21 fs. Note that these numbers are only well defined for small variations. Since they are determined as the linear component of a polynomial fit the region of its validity is limited.

The sensitivities are used to determine the tolerances. The required performance at the undulator is divided by the corresponding sensitivity to obtain the allowed deviation of a single jitter source to cause the allowed error, assuming all other sources to be stable (compare Eq. 1). Since some components are driven by uncorrelated jitter sources, such as for the linac RF stations, one can take the square root of the number of independent sources (4 klystrons for the S-band linac, 8 klystrons for the C-band linac 1, and 7 sources for C-band linac 2 and 11 RF stations in linac 3).

The jitter budget at the undulator entrance is determined from the SASE dynamics. Intrinsic fluctuations of the FEL process can be used to define the tightest tolerances. Stabilising the beam on a level below this intrinsic fluctuations

Table 2: Sensitivities of beam performance with respect to different parameters of the linac (see first column). The sensitivities of different beam properties (columns) are represented for different machine parameters (lines).

| | $\Delta t$ [fs] | $I_{\text{peak}}$ [%] | $\Delta E$ [%] |
|---|---|---|---|
| SBP [deg] | -210 | -44 | -0.32 |
| SBA [rel] | -3.9e+004 | +3.9e+004 | -93 |
| XBP [deg] | +0.68 | +82 | -0.058 |
| XBA [rel] | +3.9e+003 | -3e+003 | +8.6 |
| L1P [deg] | -370 | -170 | +0.33 |
| L1A [rel] | -5.6e+004 | -3.4e+003 | +31 |
| L2P [deg] | +0.01 | +0.084 | +5.9e-005 |
| L2A [rel] | +340 | -15 | +26 |
| L3P [deg] | +0.014 | +0.093 | +5.6e-005 |
| L3A [rel] | +550 | -86 | +41 |
| LHQ [pC] | +1 | -2.7 | +0.0011 |
| LHt [fs] | -0.032 | +0.073 | +1.7e-005 |
| LHE [rel] | -2.1e+004 | +1.6e+004 | -45 |
| BC1 [rel] | +390 | +4.7e+003 | -3.5 |
| BC2 [rel] | -110 | +4.4e+003 | -3.2 |

Table 3: Tolerances to ensure that FEL beam fluctuations stay within acceptable limits. For each electron bunch property at the undulator entrance (columns), there is a corresponding tolerance budget for every linac component (lines). The tightest given tolerance from different performance requirements are marked as bold. Unreasonable high values are given in italic.

| | $\Delta t$ [fs] | $I_{\text{peak}}$[%] | $\Delta E$[%] |
|---|---|---|---|
| goals: | 20 | 5 | 0.05 |
| SBP [deg] | **0.19** | 0.23 | 0.32 |
| SBA [rel] | 0.001 | **0.00026** | 0.0011 |
| XBP [deg] | *30* | **0.061** | 0.86 |
| XBA [rel] | 0.0051 | **0.0017** | 0.0058 |
| L1P [deg] | 0.15 | **0.084** | 0.43 |
| L1A [rel] | **0.001** | 0.0041 | 0.0046 |
| L2P [deg] | *5.2e+003* | *1.6e+002* | *2.2e+003* |
| L2A [rel] | **0.15** | 0.87 | 0.0051 |
| L3P [deg] | *4.6e+003* | *1.8e+002* | *2.9e+003* |
| L3A [rel] | **0.12** | 0.19 | 0.0041 |
| LHQ [pC] | 19 | **1.9** | 47 |
| LHt [fs] | 6.2e+002 | **68** | 2.9e+003 |
| LHE [rel] | 0.00097 | **0.00031** | 0.0011 |
| BC1 [rel] | 0.052 | **0.0011** | 0.014 |
| BC2 [rel] | 0.19 | **0.0011** | 0.015 |

will not improve machine performance, namely the FEL photon pulse stability. This defines the level of allowed peak current fluctuations to 5%, which is the result of a series of Genesis [6] runs. Beam arrival time is assumed to be on the order of the photon pulse length. A jitter of 0.05% in the mean energy would keep the resonant condition within the FEL bandwidth. Table 3 gives a summary of these tolerances. The numbers given in Table 3 represent the value by which a certain value can jitter to exhaust the tolerance goal. For example: To get 5% peak current stability, the C-band linac 1 phase should be stable within 0.084 degree rms. Please note that some values are unreasonable large. This is an effect from the linear fit as discussed earlier. In some cases the linear sensitivities are very low. As a result the tolerances defined by Eq. 1 are outside an interval where the linear approximation is valid. These values are marked in italic letters.

FEL light users might accept larger FEL jitter, which would relax the given beam tolerances by the same factor.

One remark to the injection time at the laser heater: ASTRA calculations show that an arrival time jitter of the laser on the cathode of 1fs will result in an injection time jitter of 0.81 fs at the laser heater. Therefore the value of 68 fs from Table 3 corresponds to a 85 fs allowed laser timing jitter on the cathode.

Finally, to estimate the total stability of the electron beam at Aramis, we use expected jitter from the subsystems (summarised in Tab. 4), multiplied by the sensitivities and the square root of the number of independent sources. At the SwissFEL Injector Test Facility [3] preliminary measurements at the S-band system show a shot-to-shot rms stability of 0.02 deg for the phase and $2 \cdot 10^{-4}$ for the amplitude.

In this way, the contribution of each source to the final jitter is calculated. We assume uncorrelated jitter between the different sources, and therefore the total jitter is determined as their quadratic sum. A summary of these numbers is given in Fig. 2.

## SUMMARY AND OUTLOOK

A new working point with relaxed requirements for the RF systems of SwissFEL is presented here. This is done with the same hardware layout and similar beam parameters at the end of the machine. Mainly the decoupling of the chirp generation for the two compressor stages and in general a higher compression factor in the second chicane causes the relaxed tolerances. We want to point out that a layout was defined following the described decoupling strategy and that it successfully relaxed the tolerances but not necessarily that we reached an optimal working point.

As a summary of Table 3 it can be said that the most critical stability requirements are imposed by the peak current stability goal. Namely these are the S- and X-band requirements. In the downstream linac amplitude stability is important in terms of the arrival time instability.

With the expected performance summarised in Table 4

Table 4: Expected performance of various subsystems of the SwissFEL. From this the beam behaviour at the Aramis undulator entrance is determined and summarised in Fig. 2

| | Expected performance |
|---|---|
| SBP [deg] | 0.015 |
| SBA [rel] | 0.00012 |
| XBP [deg] | 0.06 |
| XBA [rel] | 0.00012 |
| L1P [deg] | 0.03 |
| L1A [rel] | 0.00012 |
| L2P [deg] | 0.03 |
| L2A [rel] | 0.00012 |
| L3P [deg] | 0.03 |
| L3A [rel] | 0.00012 |
| LHQ [pC] | 2 |
| LHt [fs] | 30 |
| LHE [rel] | 0.0001 |
| BC1 [rel] | 5e-005 |
| BC2 [rel] | 5e-005 |

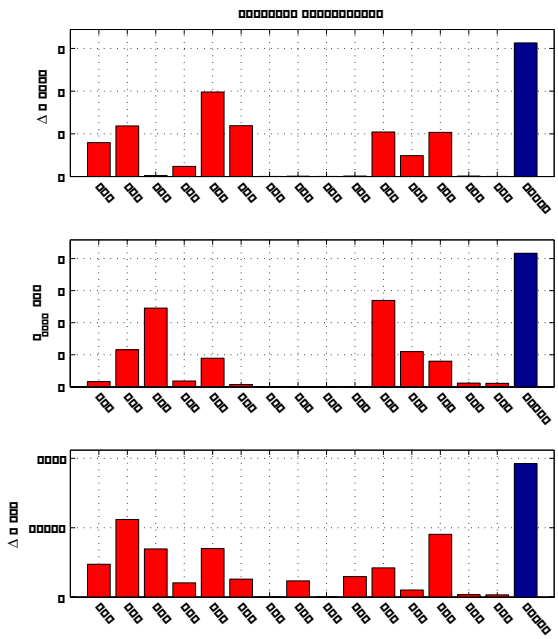

Figure 2: Electron beam jitter at Aramis entrance, assuming some jitter sources (listed in Tab. 4). The red bars give the contribution of each individual subsystem while the blue bars represent their total. The total performance is 6.3 fs arrival time fluctuations, 8.3% peak current jitter, and 0.0096% energy stability. For comparison the ultimate goals are 20 fs arrival time, 5% peak current, and 0.05% energy stability.

and Figure 2 it is shown that the arrival time and energy stability goal is reached with the assumed component stability.

The peak current stability is not reached. A stability performance in peak current of 8.3% is reached compared to the 5% goal. The main driver is the initial charge jitter and the X-band phase stability. In the expected stability performance of Table 4 a charge jitter of 2pC at 200pC is assumed. However, at the SwissFEL Injector Test facility [3] a laser stability performance of 0.5% at 200pC was demonstrated. For the second main reason of peak current jitter, the X-band phase, further optimisation of this is possible. Similar to the design of LCLS the X-band cavity should not be operated around the 180 deg point but about 20 deg shifted from that. In such a situation the generated chirp is more stable with respect to phase jitter and the chirp for BC1 is partially generated in the X-band which relaxes the phase stability requirements for the S-band booster.

As a final remark we would like to point out that the 5% goal for peak current stability at the undulator entrance is the tightest reasonable goal. The intrinsic variation of the SASE FEL provides a jitter in the photon number of about the same magnitude. However, for most users of FEL radiation a measurement of each photon pulse power on a percent level or better is mandatory. With such a photon pulse energy measurement available the requirements on the actual shot-to-shot stability are reduced because it is possible to sort and bin the data for the measured intensities.

Please note that the tolerances given here are only valid if only one source is instable at a given time. A final step in this analysis is a determination and optimisation of weighting factors as outlined in Eq. 3 and 4 in collaboration with experts of the hardware of the subsystems based on the numbers presented in Tab. 3.

## ACKNOWLEDGEMENTS

Valuable contributions and fruitful discussions for this paper from Paul Emma, Florian Loehl, Rasmus Ischebeck, Romain Ganter, Yujong Kim, and Martin Dohlus are acknowledged.

## REFERENCES

[1] R. Ganter et al, SwissFEL Conceptual Design Report, PSI-Bericht 10-04

[2] Y. Kim *et al.* "Beam Diagnostics and RF Systems Requirements for the SwissFEL Facility", Proceedings of DIPAC09, Basel, Switzerland

[3] M. Pedrozzi at al, 250 MeV Injector Concept Report. Accelerator test facility for SwissFEL, PSI-Bericht 10-05

[4] K. Flöttmann. Astra User Manual. http://www.desy.de/~mpy/astra_dokumentation.

[5] M. Borland, "elegant: A Flexible SDDS-Compliant Code for Accelerator Simulation," Advanced Photon Source LS-287, September 2000.

[6] S. Reiche, Nucl. Inst. & Meth. **A429** (1999) 243